

# A simple guideline to apply excitation-emission matrix spectroscopy (EEMs) for the characterization of dissolved organic matter (DOM) in anoxic marine sediments

Shuchai Gan<sup>1\*</sup>, Verena B. Heuer<sup>1</sup>, Frauke Schmidt<sup>1</sup>, Lars Wörmer<sup>1</sup>, Kai-Uwe Hinrichs<sup>1</sup>

<sup>1</sup> MARUM—Center for Marine Environmental Sciences, University of Bremen, Bremen D-28359, Germany

Received 25 January 2022; accepted 25 April 2022

© Chinese Society for Oceanography and Springer-Verlag GmbH Germany, part of Springer Nature 2023

## Abstract

Marine sediments represent a major carbon reservoir on Earth. Dissolved organic matter (DOM) in pore waters accumulates products and intermediates of carbon cycling in sediments. The application of excitation-emission matrix spectroscopy (EEMs) in the analysis of subseafloor DOM samples is largely unexplored due to the redox-sensitive matrix of anoxic pore water. Therefore, this study aims to investigate the interference caused by the matrix on EEMs and propose a guideline to prepare pore water samples from anoxic marine sediments. The parameters determined by fluorescence spectra include 3D-index derived from EEMs after parallel factor analysis (PARAFAC), fluorescence index (FI) (contribution of terrigenous DOM), biological index (BIX) and humification index (HIX) derived from 2D emission spectra. First, we investigated the impacts of extensively-presented ions as typical electron acceptors, which are utilized by anaerobic microbes and stratified in marine sediments: Fe(II), Fe(III), Mn(II) and sulfide in anoxic pore water resulted in biases of fluorescent signals. We proposed threshold concentrations of these ions when the interference on EEMs occurred. Effective removal of sulfide from sulfide-rich samples could be achieved by flushing with N<sub>2</sub> for 2 min. Second, the tests based on DOM standard were further verified using pristine samples from marine sediments. There was a significant change in the fluorescence spectra of DOM in anoxic sediments from the Rhône Delta. This study demonstrated that the change was caused by oxidation of the matrix rather than the intrinsic alteration of DOM. It was confirmed by extracted DOM via both EEMs analysis and Fourier transform ion cyclotron resonance mass spectrometry (FT-ICR-MS). Slight oxidation of sulfur-containing compounds (e.g., sulfhydryl) and polyphenol-like compounds occurred. Finally, a sample preparation sequence is proposed for pore water from anoxic sediments. This method enables measurement with small volumes of the sample (e.g., 50 µL in this study) and ensures reliable data without the interference of the redox-sensitive matrix. This study provides access to the rapid analysis of DOM composition in marine sediments and can potentially open a window into examining the carbon cycling of the marine deep biosphere.

**Key words:** marine subsurface sediment, EEMs, PARAFAC, FT-ICR-MS, anaerobic pore water

**Citation:** Gan Shuchai, Heuer Verena B., Schmidt Frauke, Wörmer Lars, Hinrichs Kai-Uwe. 2023. A simple guideline to apply excitation-emission matrix spectroscopy (EEMs) for the characterization of dissolved organic matter (DOM) in anoxic marine sediments. *Acta Oceanologica Sinica*, 42(1): 109–119, doi: 10.1007/s13131-022-2050-0

## 1 Introduction

Marine sediments and sedimentary rocks play a key role in the global carbon cycle as the largest carbon pool on Earth (Bernier, 1982, 1990; Hedges and Keil, 1995). Sediments contain both particulate organic matter (POM) and dissolved organic matter (DOM) in their interstitial waters. Since turnover rates are slow, alterations in the large POM pool are difficult to observe, but organic matter degradation might be observable in the much smaller, more short-lived DOM pool. As an intermediate pool during the remineralization of sedimentary organic matter, DOM receives the products of hydrolysis and fermentation processes, thus holding the pool of substrates accessible to terminal remineralization (Middelburg et al., 1993). Detailed analyses of sedimentary DOM can potentially open a window into the examination of carbon cycling and thereafter marine deep biosphere in

sediments (Krom and Sholkovitz, 1977; Chin et al., 1998; Weston et al., 2006; Tfaily et al., 2013; Valle et al., 2018).

Marine sedimentary DOM is a complex mixture of thousands of distinct compounds (Schmidt et al., 2009, 2011). Concentrations of bulk dissolved organic carbon (DOC) and individual volatile compounds have been determined routinely in the context of scientific ocean drilling programs (Simoneit and Sparrow, 2002; Heuer et al., 2009; Lin et al., 2012, 2015; Zhuang et al., 2014), but an overall characterization of the complex DOM pool and the profile distribution of DOM in deep sediments has rarely been achieved.

Fluorescence spectroscopy can be carried out on smaller sample volumes (2–3 mL for seawater) without pretreatment by solid phase extraction (SPE), is non-destructive and inexpensive. It takes advantage of the presence of chromophores in DOM that

Foundation item: The European Union's Seventh Framework Programme—Ideas Specific Programme under contract No. 247153 (Advanced Grant DARCLIFE; Principal Investigator, K.-U.); the Fund of the Deutsche Forschungsgemeinschaft through the Research Center/Excellence Cluster MARUM—Center for Marine Environmental Sciences, Project GB2; the Fund of China Scholarship Council; the Fund of Bremen International Graduate School for Marine Sciences.

\*Corresponding author, E-mail: [ganshuchai@scbg.ac.cn](mailto:ganshuchai@scbg.ac.cn)

absorb and emit light of specific wavelengths, which are related to the molecular structure of the compounds. 3D fluorescence spectrum, generated by excitation-emission matrix spectroscopy (EEMs), contains thousands of excitation and emission wavelength-dependent data points of fluorescence intensity that can be grouped into different DOM components by parallel factor analysis (PARAFAC) as a statistical tool (Stedmon and Bro, 2008; Murphy et al., 2010, 2013; Cuss and Guéguen, 2016). EEMs can be used to identify and quantify different fluorescent DOM components such as protein-like peaks related to labile compounds (Yamashita and Tanoue, 2003; Stedmon and Markager, 2005; Fellman et al., 2010; Lønborg et al., 2010), and humic-like peaks indicating highly aromatic terrestrial DOM, microbial or marine DOM (Coble, 1996, 2007; Fellman et al., 2010; Ishii and Boyer, 2012). Based on the individual peaks identified in 3D scans, peak ratios can be used to infer the aromaticity, sources and bioavailability of DOM without determination of the exact molecular composition. In addition, 2D-scans of emission spectra resulting from excitation at 370 nm, 310 nm, and 254 nm serve as index for the terrestrial source (fluorescence index: FI), biological source (biological index: BIX) and degree of humification (humification index: HIX), respectively (McKnight et al., 2001; Ohno, 2002; Huguet et al., 2009). More indices can be derived from 3D-scans and 2D-scans, e.g., peak ratios (Baker et al., 2008; Hansen et al., 2016).

EEMs have been successfully applied to investigate DOM in the water column of oceans, estuaries and rivers (Coble, 2008; Yamashita et al., 2008; Jiang et al., 2009; Murphy et al., 2010; Lønborg et al., 2010; Guo et al., 2010; Yi et al., 2014; Gan et al., 2016; Wang et al., 2019), and marine surface sediments (Burdige, 2001; Komada et al., 2002; Burdige et al., 2004). The DOM composition indicated by fluorescence spectra has been reported in former studies of porewater at a depth of less than 30 cm in lacustrine sediments (Wolfe et al., 2002; Chen and Hur, 2015; Huang et al., 2015; Guillemette et al., 2017). However, the suitability of extraction procedures to obtain a surrogate of DOM remains ambiguous (Rennert et al., 2007). It is suggested that oxygen affects DOM in anoxic pore waters and that caution is needed in manipulating the samples (Chen and Hur, 2015). However, it is not clear which component of DOM and how the interpretation of EEMs are affected by oxygen. The applicability and handling of EEMs for DOM in anoxic marine subsurface sediments are largely unexplored. In particular, the following matrix and sample handling effects require attention compared to the aquatic systems or surface sediments. (1) Concentrations of iron and other metal ions in anoxic deep sediments could be as high as 0.5 mmol/L, which is much higher than the surface sediment and seawater. It might lead to complexation of DOM components and possibly to precipitation or coagulation, thus affecting chromophore properties and identification of EEMs peaks. For example, iron-quenching effects on fluorescence spectra have been shown (Poulin et al., 2014). It is important to identify at which concentration range the ions might interfere with the EEMs. (2) Anoxic conditions prevail in deep marine sediments, and the contact of sedimentary DOM samples with ambient air during sample handling and storage might trigger oxidation, complexation, and precipitation that can affect optical signals.

Therefore, this study aims to explore the applicability of EEMs for DOM characterization in marine seafloor sediments by establishing the pretreatment guidelines and evaluating the applicability of EEMs in viable sedimentary matrices. We investigated the potential matrix effects in sediment pore-waters in a series of experiments, including major redox-sensitive metal ions and  $S^{2-}$ .

Suwanee River Fulvic Acid Standard (SRFA) and yeast extract (YE) were tested as the representatives for humic-like and protein-like DOM, respectively, as well as two natural sedimentary DOM prepared from slurries of coastal marine sediments after anoxic incubations (North Sea tidal flat and Rhône Delta). The anoxic natural samples were used to test the effect of oxygen exposure during sample handling for EEMs and FT-ICR-MS analyses.

## 2 Materials and methods

### 2.1 Experiments

#### 2.1.1 Preparation of stock solutions and test of matrix effects in DOM samples prepared from SRFA and YE standards

Potential matrix effects that might occur in marine sedimentary DOM due to high concentrations of DOM, salts, metals and sulfide in pore water were tested with two reference samples. Humic-like DOM was investigated using a 1 g/L stock solution prepared from SRFA (standard reference material of the International Humic Substances Society) dissolved in  $O_2$ -free Milli-Q water and flushed with  $N_2$ . Protein-like DOM was investigated using a 10 g/L stock solution, which had been prepared from YE (H26769, Alfa Aesar) in  $O_2$ -free Milli-Q water. Both solutions were kept under  $N_2$  atmosphere in 100-mL serum bottles that were closed with grey butyl rubber stoppers and crimp caps.

The impact of major redox-sensitive metal ions was tested by the addition of  $FeCl_3$ ,  $FeCl_2$ ,  $MnCl_2$ , yielding a concentration range of 0–0.9 mmol/L for the metal ions and a DOM concentration of 1.8 mg/L (in terms of C) for SRFA and 3 mg/L (in terms of C) for YE. The potential interference of sulfide was tested within a concentration range of 0–10 mmol/L in 1.8 mg/L (in terms of C) SRFA and 3 mg/L (in terms of C) YE, respectively. Stock solutions of  $Na_2S$  were prepared at a concentration of 200 mmol/L and kept under  $N_2$ . The salts solutions were made with  $O_2$ -free Milli-Q water with 2-h flushing by  $N_2$  and stored in serum bottles. The bottles were sealed with butyl rubber stoppers at a pressure of  $2 \times 10^5$  Pa in  $N_2$  headspace to avoid intrusion of air. During measurements, the quartz cell with full solution and cap was placed in air atmosphere. All dilution series were prepared on the same day in  $O_2$ -free Milli-Q water and analyzed immediately by fluorescence spectrometry.

#### 2.1.2 Preparation of fresh slurries for simulating the matrix effects of natural marine sedimentary DOM

In order to confirm the matrix and sampling effects in natural anoxic pore-water samples, two in-house standards of marine sedimentary DOM were prepared using large samples of surface sediment from two contrasting environments—a North Sea tidal flat and the prodelta of the River Rhône. While the former has low total organic carbon (TOC=0.1%) and high sulfide concentrations (3.95 mmol/L after incubation), the latter is characterized by high concentrations of TOC and metals. The first in-house standard was prepared from surface sediment (~2–7 cm) of the tidal flat Janssand off Spiekeroog Island, North Sea (53°44.18'N, 7°41.97'E), that was accessed by foot during ebb tide in October 2013. The coastal sediment was sandy, black, and odorous due to a high abundance of dissolved sulfide. The TOC content (mass fraction) was low (0.1%) (Wu et al., 2018). The sediment was representative of natural sulfide-enriched autochthonous DOM samples. The second in-house standard (Rhône Delta) was prepared from surface sediments (mixtures of sediments from a depth of 0–18 cm) from the Rhône Delta in the Gulf of Lions,

western Mediterranean Sea, sampled at Site GeoB17306 (43°18.95'N, 4°52.18'E, 30 m water depth) during the R/V *Posidon* Cruise POS450 in April 2013. This coastal site is characterized by high riverine input, high TOC content (mass fraction) (1.3%–1.4%), anoxic conditions, and high concentrations of dissolved metal ions ( $\text{Fe}^{2+}$ : 45–426  $\mu\text{mol/L}$ ) (Schmidt et al., 2017). This sample represents a typical terrestrial DOM end member dominated by humic-like compounds with slight admixture of protein-like compounds. The surface sediment was retrieved by multi corer (GeoB17306-1). Immediately after core recovery, the upper 0–18 cm of sediment were transferred into three Schott glass bottles, which were flushed with  $\text{N}_2$ , closed with butyl rubber stoppers and stored at +4°C until further processing onshore. Details on coring operations and sample handling onboard are given in the cruise report (Heuer et al., 2014).

To generate fresh large-volume aqueous samples for DOM analysis, the sediment samples were homogenized and further processed in the following way: 100 mL of wet sediment were slurried 1:1 with oxygen-free autoclaved artificial seawater (Gan et al., 2020). The slurries were kept under  $\text{N}_2$  atmosphere in 250-mL Schott glass bottles closed with butyl rubber stoppers, and incubated in the dark at room temperature for one year for the samples from the Rhône Delta and two years for the samples from the North Sea. For the slurry of the latter, 20-mL liquid was taken and filtered through  $\text{N}_2$ -flushed acetate cellulose filter (Sartorius, 0.2  $\mu\text{m}$ ), samples were used for test of precipitation, oxidation and removal of sulfide. The rest of the slurry after two-year incubation was incubated at 85°C for 15 d as representative of natural DOM samples containing both protein-like and humic-like compounds due to the release of high proportions of peptides in the heated sediment (Lin et al., 2017). After incubation, the liquid phase was sampled by syringe and filtered through  $\text{N}_2$ -flushed acetate cellulose filter (Sartorius, 0.2  $\mu\text{m}$ ) prior to further processing, storage or analysis. For FT-ICR-MS analysis, 20-mL samples of the filtered liquid phase were stored in glass serum vials under  $\text{N}_2$  atmosphere at +4°C.

The original concentration of dissolved organic carbon in the incubated slurries is 36 mg/L (in terms of C) and 60 mg/L (in terms of C) for samples from the Rhône Delta and North Sea, respectively.

### 2.1.3 Effects of sample storage on DOM samples from anoxic slurries

While EEMs can be conducted at the time of sampling without further sample treatment, FT-ICR-MS requires sample preparation by SPE (Dittmar et al., 2008), and usually the limited access to the analytical infrastructure requires sample storage. Here, we tested (1) the effect of short-term  $\text{O}_2$  exposure of

pristine liquid phase of the in-house-prepared DOM samples on the results of EEMs, and (2) the effect of long-term  $\text{O}_2$  exposure on DOM samples after SPE on the results of FT-ICR-MS and, for comparison, on the results of EEMs. In the latter test, the reported change of FT-ICR-MS data and EEMs of DOM after SPE refers to only the variation of DOM without the matrix effects of inorganic ions.

SPE of DOM was performed on 20-mL liquid phase samples using pre-cleaned Bond Elut-PPL cartridges (200 mg sorbent, Agilent Inc.) according to Dittmar et al. (2008) and Schmidt et al. (2014). Extraction was carried out in a glove bag under  $\text{N}_2$  atmosphere. DOM was eluted from the cartridge with 1.5-mL methanol (LiChrosolv, Merck). The residue sample passing through the SPE column and losing extractable DOM was sampled and neutralized to check the loss of fluorescence signal during solid phase extraction. The DOM extracts of both in-house standards for FT-ICR-MS and EEMs analysis were further split into two parts and stored for two months at –20°C, one under ambient air and the other under  $\text{N}_2$  atmosphere. For storage, we used 2-mL glass vials closed with Teflon coated septa. To ensure  $\text{O}_2$ -free storage conditions, the 2-mL sample vials were kept in  $\text{N}_2$  flushed 50-mL Schott bottles. DOM extracts after SPE were analyzed by FT-ICR-MS. For EEMs measurements, 20- $\mu\text{L}$  DOM extracts in methanol were taken, dried, and dissolved in  $\text{O}_2$ -free Milli-Q water.

In addition, the original liquid phase of the in-house-prepared samples from the Rhône Delta and North Sea sediments was measured by fluorescence spectrometer prior to  $\text{O}_2$  exposure, after 2-h and 24-h  $\text{O}_2$  exposure. All the experiments are summarized in Table 1 and Fig. S1.

## 2.2 Analytical methods

### 2.2.1 EEMs

Spectra were recorded by a fluorescence spectrophotometer (Agilent Cary Eclipse, USA). The integral area of the Raman peak at excitation 350 nm was determined using Milli-Q water as a reference. Excitation wavelengths were increased in 5 nm steps from 230 nm to 410 nm, and emission spectra were recorded in 2 nm intervals from 300 nm to 530 nm. The EEMs were subtracted by blank to remove Raman and Rayleigh peaks. There were 275 samples in the final dataset for PARAFAC processing (Stedmon and Bro, 2008). The relative standard deviation of the Raman peak excited at 350 nm was below 0.5% from a routine measurement tested with fresh Milli-Q water. The reproducibility test of 1.8 mg/L (in terms of C) SRFA suggests that the relative standard deviation of peaks modeled by PARAFAC was better than 2%. The spectra with significant loss of signal or uncommon peaks resulting from the addition of metal ions were deleted dur-

**Table 1.** Summary of main subseries experiments and controls

Experiment	Sample, matrix or treatment	Purpose of tests
Incubation of sediments	North Sea sample (20°C)	sulfide-rich samples
	North Sea sample (85°C)	samples enriched in protein-like compounds and humic-like compounds
	Rhône Delta sample (20°C)	
Matrix effects	$\text{S}^{2-}$	impacts of anions involved in anoxic mineralization
	Mn(II), Fe(II), Fe(III)	impacts of metal ions involved in anoxic mineralization
	matrix-removed DOM	method to avoid matrix effects
Storage effects	DOM extracts, $\text{O}_2$ exposure	oxidation of DOM
	pristine samples, Rhône	impacts of matrix oxidation during storage under $\text{O}_2$ and method to avoid storage effects
	pristine samples, North Sea	

Note: The pristine sample refers to original pore water without solid phase extraction (SPE); the dissolved organic matter (DOM) extracts refer to purified sample without inorganic matrix after SPE.

ing the PARAFAC processing analysis as they induced unsuccessful split-half analysis. Afterwards, the five-component model was validated by split-half analysis (Stedmon and Bro, 2008) (Fig. S2). The results of PARAFAC analysis were compared with other studies via the online OpenFluor library (Murphy et al., 2014) and presented in Fig. S3 in the supplementary materials (congruence threshold, 0.95). For the dilution series (Figs S4 and S5), we diluted the samples with oxygen-free Milli-Q water, the quartz cell was fully filled with diluted solution and sealed with cap without headspace.

Absorption spectra were measured on a Shimadzu UV-1280 UV-vis absorption spectrophotometer with a 1-cm cuvette. Absorption at wavelength 350 nm was recorded. Absorption measured in the machine (abs) could be transformed to the absorption coefficient ( $a_{350}$ ) by the equation:

$$a_{(\lambda)} = 2.303A_{(\lambda)}/L, \quad (1)$$

where  $L$  is the cell path-length in meters,  $\lambda$  is the wavelength,  $A$  is measured absorbance. Absorption spectra were measured to quantify the concentration of CDOM. The upper limit of absorption coefficient is  $10 \text{ m}^{-1}$  (Stedmon and Bro, 2008) when inner filter effects occur.

### 2.2.2 2D-scans

2D emission spectra were recorded at excitation 254 nm, 310 nm and 370 nm, respectively. The index FI, BIX and HIX derived from 2D-scans of emission spectra were interpreted as proxies of terrestrial organic matter source (FI), biological activity (BIX) and humification (HIX), respectively (McKnight et al., 2001). FI was determined as the ratio of the fluorescence intensity at 450 nm to 500 nm emission excited at 370 nm, indicating terrestrial-derived DOM (derived from higher terrestrial plant) with FI of less than 1.4 and microbial-derived DOM with FI of more than 1.8 (McKnight et al., 2001). BIX is the ratio of fluorescence intensity emitted at 380 nm and the maximum of intensity at 430 nm excited at 310 nm, indicating fresh autochthonous DOM production (BIX > 1) (Huguet et al., 2009). HIX is calculated as the ratio of integrated fluorescence emission in the range of 435–480 nm ( $\Sigma I_{435-480}$ ) to that in the range of 300–345 nm ( $\Sigma I_{300-345}$ ), indicating humified DOM with HIX higher than 10 and autochthonous DOM with HIX less than 4 (Zsolnay et al., 1999; Huguet et al., 2009). HIX above 10 indicates humified DOM. High HIX values correspond to maximal fluorescence intensity at long wavelengths and thus to the presence of complex molecules such as high-molecular-weight aromatics (Senesi et al., 1991; Zsolnay et al., 1999; Huguet et al., 2009).

### 2.2.3 FT-ICR-MS

Samples subjected to SPE were measured by FT-ICR-MS. Samples were analyzed in methanol/water 1:1 (volume ratio) with negative-ion electrospray ionization (ESI, Apollo II electrospray source, Bruker Daltonik GmbH, Bremen, Germany) with a flow rate of 5  $\mu\text{L}/\text{min}$  on a Bruker Solarix XR FT-ICR-MS (Bruker Daltonik GmbH, Bremen, Germany) equipped with a 7 T refrigerated actively shielded superconducting magnet (Bruker Biospin, Wissembourg, France). Sodium trifluoroacetate was used as a calibration compound (Moini et al., 1998). DOM extracts were injected at a concentration of  $\sim 20 \text{ mg}/\text{L}$  (in terms of C). A total of 200 scans were added to one mass spectrum. The capillary voltage was 4 500 V. Details of formulae assignments were described in Schmidt et al. (2014). The peak magnitudes ( $r_{\text{Intn}}$ ) reported in this manuscript are relative intensity normalized to the

sum of all peaks, i.e.,

$$r_{\text{Intn}} = I_{\text{Peak}} / \sum I_{\text{AllPeaks}}, \quad (2)$$

Aromaticity index (AI) refers to the density of carbon-carbon double bonds in a molecule and can be calculated after Eq. (3) (Koch and Dittmar, 2006, 2016):

$$\text{AI} = \frac{1 + n_{\text{C}} - \frac{1}{2}n_{\text{O}} - n_{\text{S}} - \frac{1}{2}(n_{\text{N}} + n_{\text{P}} + n_{\text{H}})}{n_{\text{C}} - \frac{1}{2}n_{\text{O}} - n_{\text{N}} - n_{\text{S}} - n_{\text{P}}}, \quad (3)$$

where  $n$  is the number of atoms carbon (C), hydrogen (H), oxygen (O), nitrogen (N), sulfur (S) and phosphorus (P) in a molecular formula.

### 2.2.4 DOC

DOC was measured by high-temperature catalytic oxidation at 750°C (MultiN/C 2100 s, Analytik Jena). DOC was measured as non-purgeable organic carbon in acidified samples purged with  $\text{CO}_2$ -free synthetic air. Product  $\text{CO}_2$  was detected by infrared spectroscopy.

## 3 Results and discussion

### 3.1 Results of PARAFAC analysis and derived index

Based on EEMs and PARAFAC, the Peaks B, T, M, A(C), and C were identified in 3D-scan spectra and named based on the maxima of excitation and emission intensities (ex/em) (Fig. 1). Peak P represents the total protein-like DOM (including Peaks B and T, B: ex/em, 275 nm/305 nm; T: ex/em, 280 nm/350 nm). Peaks M (ex/em: 315(250) nm/400 nm), A(C) (ex/em: 250(350) nm/450–460 nm) and C (ex/em: 350 nm/450–460 nm) represent humic-like DOM. They are also grouped together as Peak H. The value given in parenthesis (250) refers to the secondary peak. Peak A(C) represents Peak A with Peak C in the PARAFAC analysis results. “AC” represents the sum of Peak A(C) and Peak C. The intensity of fluorescence is normalized by the Raman peak and the unit is R.U.

Apart from the five peaks identified after PARAFAC analysis (Fig. 1) and the index FI, BIX and HIX derived from the 2D-scan of the emission spectrum (as described above), more parameters can be derived from individual peaks. The peak height ratio of Peaks A and C to Peak M (AC/M) or Peak C to Peak M (C/M) can be used to identify a blue-shift of the fluorescent signal of organic compounds. A low AC/M ratio is attributed to a low relative fraction of conjugated compounds, for example, aromatics and double bond-bearing compounds, among others. In aquatic systems, Peak C represents a more conjugated terrestrial DOM compared to Peak M, which in studies of seawater has been recognized to comprise marine autochthonous compounds (Coble, 2007; Ishii and Boyer, 2012). The index P/H (peak height ratio of Peak P to Peak H) represents the ratio of protein-like peaks to humic-like peaks. Four representatives in different proportion of protein-like peaks and humic-like peaks were tested (Fig. 2). The protein-like and humic-like components are 0.3 R.U. and 4.43 R.U. in the North Sea sample before hot incubation, respectively. Protein-like peaks comprise roughly <15% in our natural samples from the Rhône Delta and North Sea before hot incubation, which is similar to most terrestrial or marine sedimentary DOM pool in which protein-like DOM likely comprises only a minor

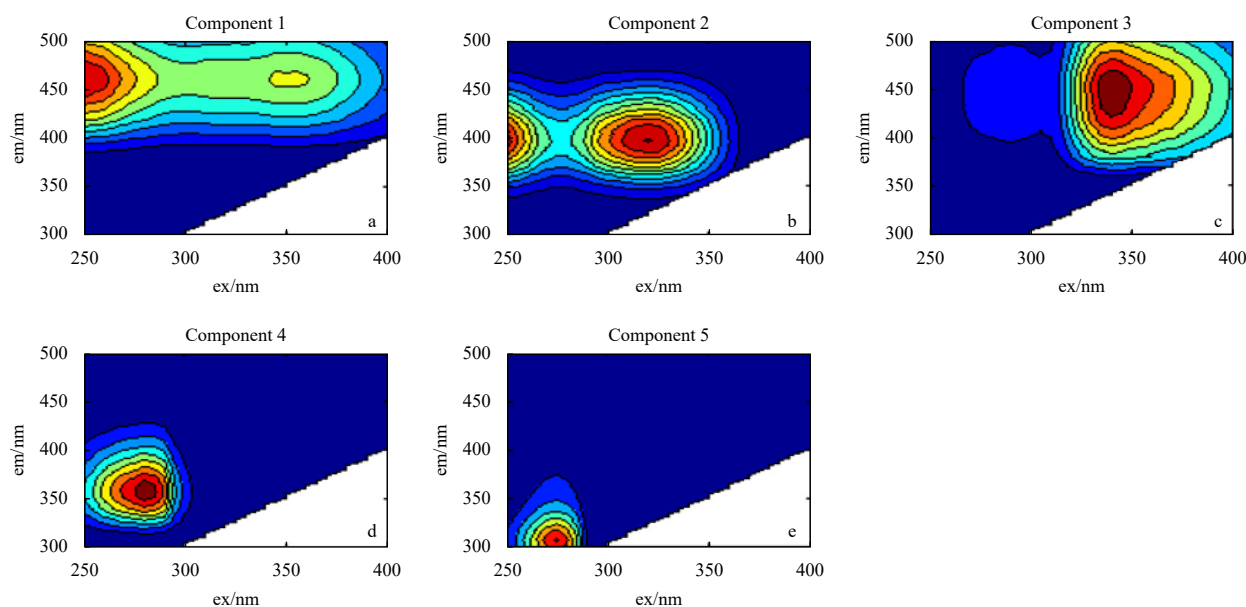


**Fig. 1.** Excitation-emission matrix spectroscopy (EEMs) components identified by parallel factor analysis (PARAFAC). Components 1, 2, 3, 4 and 5 represent Peaks A(C), M, C, T and B, respectively. More information is shown in Table S1. The em and ex represent emission and excitation wavelength, respectively.

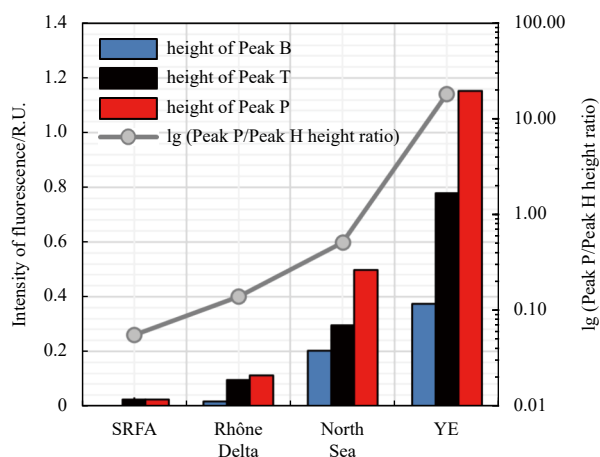


**Fig. 2.** Composition of Suwanee River Fulvic Acid Standard (SRFA), natural samples and yeast extract (YE) after parallel factor analysis.

fraction, as amino acid-C contributes <10% of DOC in pore water (Albéric et al., 1996; Lomstein et al., 1998). As for the sample from the North Sea after incubation at 85 °C, which environmentally simulates the deep biosphere in heated deep layers, fluorescence intensity of protein-like peaks is half of the humic-like peaks.

### 3.2 Experimental evaluation of potential matrix effects on EEMs

Fe(III), Mn(IV) and sulfate are important electron acceptors during organic matter degradation in marine anoxic sediment. Their reduction produces oxygen-sensitive ions such as Fe(II), Mn(II), S<sup>2-</sup>, which may affect the fluorescence spectra via the formation of metal-organic complexes and/or precipitation. Moreover, their concentration might vary due to the stratification of diagenetic processes in sediments (Canfield et al., 1993; Schulz et al., 1994). For example, as a consequence of iron reduction, up to 0.5 mmol/L dissolved iron was detected in the subsur-

face of the Rhône Delta in this study. Our results suggest that the EEMs of DOM samples are most sensitive to Fe(III): even at 0.03 mmol/L Fe(III), 40% of the fluorescence signal is lost (Table S2). High concentrations of both Fe(II) (0.2 mmol/L) and Mn(II) (0.6 mmol/L) also affect the fluorescence spectra and the derived parameters (H, AC/M, FI, HIX and BIX) (Table S2, Fig. 3). This is presumably due to the complexation between transition metal ions and organic matter (Poulin et al., 2014). One reason for the decrease of AC/M, i.e., blue-shift of fluorescence, might be that long-emission regions of the fluorescence spectra associated with greater DOM conjugation were more susceptible to iron quenching (Poulin et al., 2014). The addition of Fe(II) and Mn(II) in concentrations <0.06 mmol/L affected neither the DOM spectra nor the peaks' intensity (<5% for Fe(II), <3% for Mn(II) compared to the sample without addition) (Fig. 3). The addition of sulfide (1-mmol/L Na<sub>2</sub>S) without O<sub>2</sub> exposure in SRFA resulted in a red shift of the humic-like peaks, i.e. longer excitation and emission wavelength, and accordingly bias of AC/M, FI, BIX and HIX index (Table S2, Fig. 3).

The impact of transition metal ions and sulfide on EEMs of protein-like DOM is shown in Fig. 4 (more data in Table S2): EEMs of YE samples were slightly affected by the addition of Fe(III), Mn(II) at high concentrations of 0.2 mmol/L and 0.6 mmol/L, respectively. Compared to humic-like DOM, protein-like DOM is less sensitive to these ions. The addition of 1-mmol/L Na<sub>2</sub>S results in the loss of fluorescence intensity in protein-like peaks at low excitation wavelengths (250 nm) and a sharp increase at higher excitation wavelengths, e.g., red-shift of the spectra (Fig. 4).

### 3.3 Experimental evaluation of O<sub>2</sub> exposure effects during sample storage

For the SPE-extracted sample from the North Sea, FT-ICR-MS characterization showed a slight change in DOM after two-month O<sub>2</sub> exposure compared to storage under N<sub>2</sub> (Figs 5a, c). The few formulae in the blue dots suggest compounds with low O/C ratio (hereafter, all of the element ratios are the ratios of the

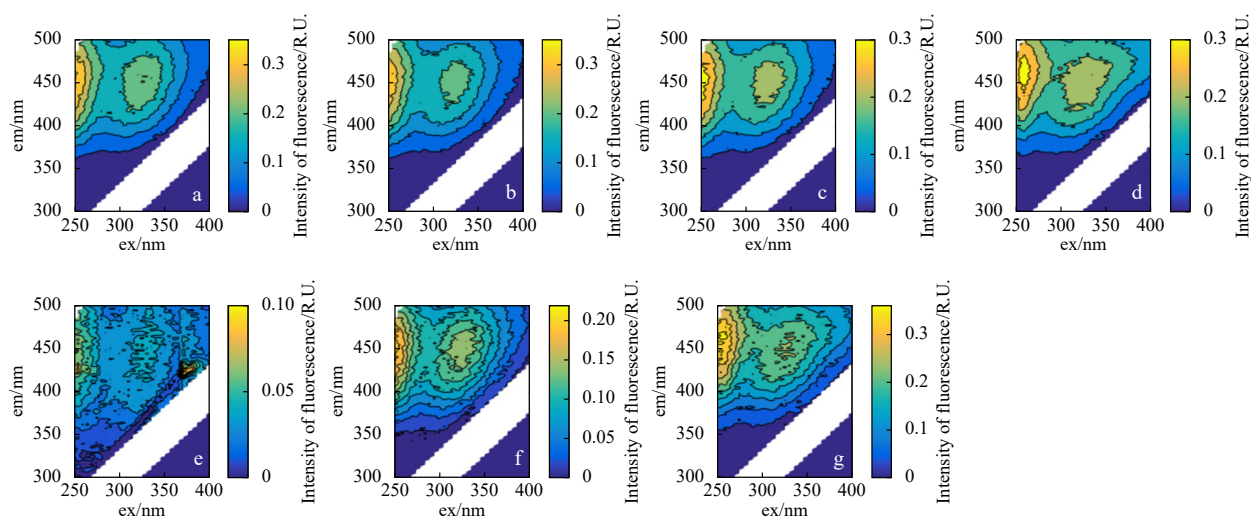


**Fig. 3.** Effect of redox-sensitive ions on humic-like peaks. a. Excitation-emission matrix spectroscopy (EEMs) spectra of original Suwannee River Fulvic Acid Standard (SRFA) samples; b–d. EEMs spectra of SRFA samples with addition of Fe(II), Mn(II), S<sup>2-</sup> at concentrations of 0.06 mmol/L, 0.06 mmol/L, 0.3 mmol/L, respectively; e–g. EEMs of SRFA samples with addition of Fe(II), Mn(II), S<sup>2-</sup> at concentrations of 0.6 mmol/L, 0.6 mmol/L, 1 mmol/L, respectively. The em and ex represent emission and excitation wavelength, respectively.

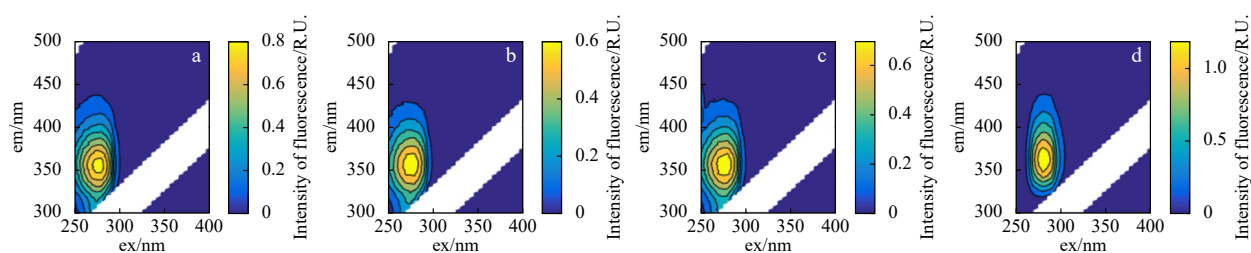


**Fig. 4.** Effect of redox-sensitive ions on protein-like peaks. a. Original excitation-emission matrix spectroscopy (EEMs) of yeast extract (YE); b–d. EEMs of YE samples with addition of Fe(III), Mn(II), S<sup>2-</sup> at concentrations of 0.2 mmol/L, 0.6 mmol/L, 1 mmol/L, respectively. The em and ex represent emission and excitation wavelength, respectively.

numbers of atoms in a molecular formula) and  $m/z$  were the most significantly transformed (Figs 5a, c): there are a total of 109 formulae decreasing by more than 0.02 in relative intensity (i.e.,  $r_{\text{intn}} > 0.00004$ ), which account for only 1.2% of all the formulae. EEMs showed consistent results: the AC/M ratio increased by 0.05 (3%) after O<sub>2</sub> exposure and the P/H ratio before and after O<sub>2</sub> exposure remained the same (0.22) for the extracted DOM (Table S2). For the extracted DOM, the quantitative change of fluorescence signals after O<sub>2</sub> exposure was not compared. The increased peak ratios of AC/M suggested that the O<sub>2</sub> exposure led to a slight red-shift of humic-like components. Consistently, the FI and the humification index increased, suggesting the formation of larger humic substances. It may be due to the oxidation of humics and the formation of larger conjugated structures with the contribution of lone pair electrons in the oxygen atom. The FI and HIX increased by 6%, indicating that care should be taken when comparing samples under different storage conditions. Marine-derived and aliphatic DOM (e.g., proteins, lipids) are less sensitive to O<sub>2</sub> exposure compared to terrestrial DOM enriched in highly unsaturated, polyphenol or tannin-like compounds.

For the SPE-extracted sample from the Rhône Delta Site Geob17306 as representative of terrestrial DOM, we observed a loss of smaller aromatic compounds ( $m/z < 400$ ) and production of larger O-rich highly unsaturated or aromatic compounds ( $m/z > 400$ ) when stored in the presence of O<sub>2</sub> (Figs 5b, d). Accord-

ing to the O/C and H/C ratios in the van Krevelen diagram, these formulae could be tannin-like polyphenol compounds (Fig. 5b). A possible mechanism involves the formation of more conjugated quinone or phenol ethers from phenolic structures in oxygen-sensitive organic compounds, resulting in longer linear macromolecules after oxygen exposure (Poncet-Legrand et al., 2010). This phenomenon is especially pronounced in the marine sediment with substantial terrestrial organic matter and polyphenols or lignin-derived compounds. More specifically, the larger O-rich formulae increased by more than 0.02 ( $r_{\text{intn}} > 0.00004$ ) in relative intensity (Figs 5b, d) and accounted for 1.2% of all assigned CHO formulae and 0.05% of all CHNO formulae (data not shown in figures). CHOS formulae were more sensitive to O<sub>2</sub> exposure, 8.9% of all CHOS formulae increased in  $r_{\text{intn}}$  by more than 0.02 ( $r_{\text{intn}} > 0.00004$ ). This is possibly due to the oxidation of sulfur-containing functional groups, e.g., sulfhydryl groups (De Filippis and Scarsella, 2003).

Without SPE, the original DOM sample from the Rhône Delta showed a recognizable change of EEM spectra (Figs 6a, b) after only 2 h of exposure to O<sub>2</sub>; at the same time, the pellucid liquid became turbid. As extracted DOM formulae remained basically unchanged after O<sub>2</sub> exposure, the distinct change of fluorescence spectra might be caused by the oxidation of redox-sensitive metal ions in the original sample. The formation of small particles of metal oxides might induce quenching of fluorescence (Man-

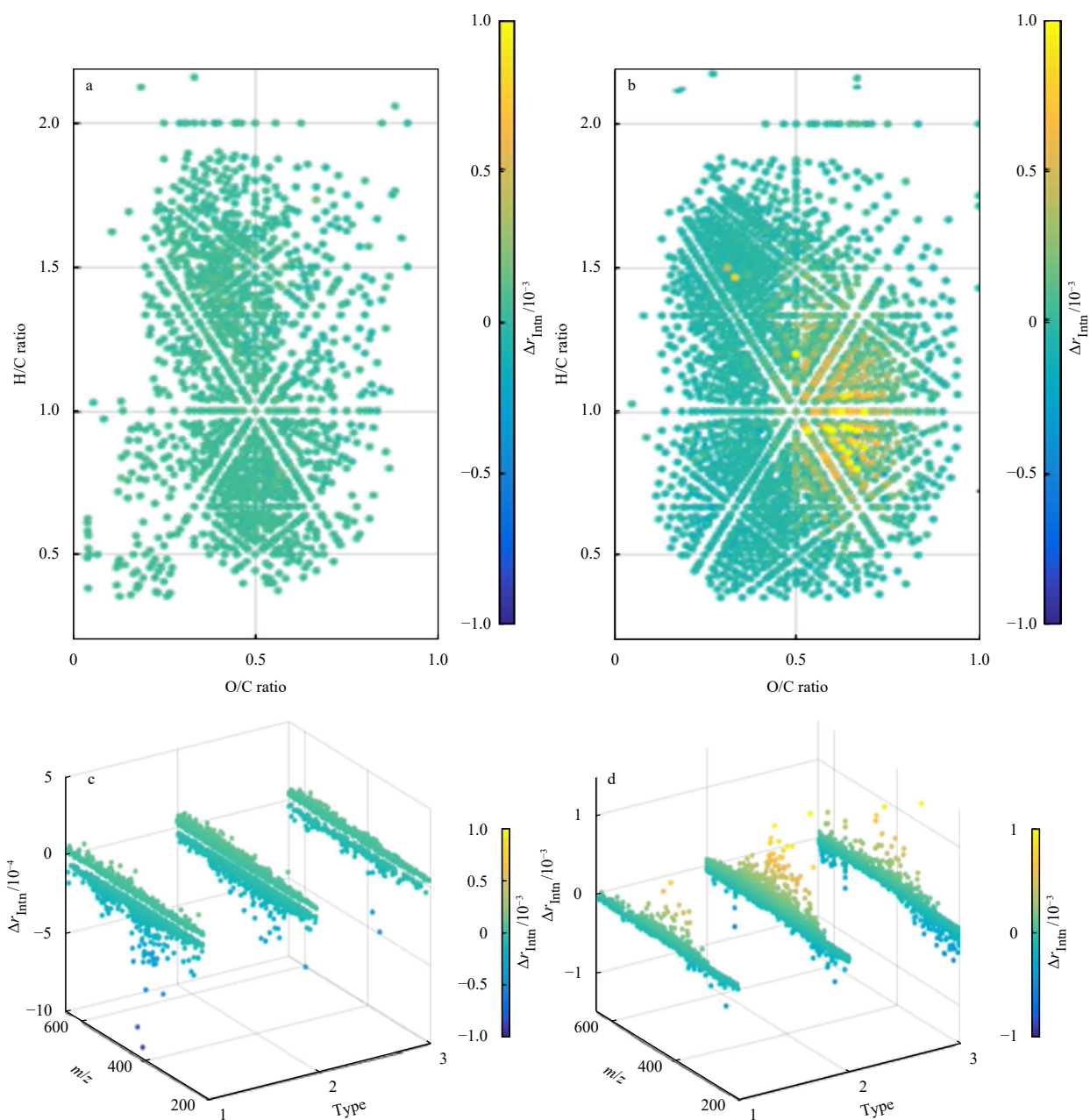


**Fig. 5.** Effect of two-month  $O_2$  exposure on pore water dissolved organic matter (DOM) characterized by FT-ICR-MS. Change of DOM sample from the North Sea (a) and Rhône Delta (b) in van Krevelen diagram; change of O/C ratio in DOM sample from the North Sea (c) and Rhône Delta (d). Type 1: aliphatic compounds,  $AI < 0$ ; Type 2: highly unsaturated compounds,  $0.5 \geq AI \geq 0$ ; Type 3: aromatic compounds (including condense aromatic compounds),  $AI > 0.5$ . The peak magnitude shown in the figure is relative intensity normalized to the sum of all peaks, i.e.,  $r_{\text{Inntn}} = I_{\text{Peak}} / \sum I_{\text{allPeaks}}$ . The color represents the difference of  $r_{\text{Inntn}}$  after air exposure ( $\Delta r_{\text{Inntn}}$ ), i.e.,  $r_{\text{Inntn-end}} - r_{\text{Inntn-start}}$ .  $r_{\text{Inntn}} > 0$ : relative abundance of formulae increases after air exposure. The y-axis in c and d shows the difference of  $r_{\text{Inntn}}$  at a narrower range. The definition of AI refers to Eq. (3).

ciulea et al., 2009). As a comparison, for the sulfide-enriched North Sea tidal flat sample without high concentrations of the redox-sensitive metal ions, EEMs were similar before and after  $O_2$  exposure for 24 h (Table S2).

### 3.4 Recommendations for the analysis of anoxic interstitial water DOM by EEMs

Our study confirms that the EEMs analysis of DOM in anoxic interstitial waters is potentially affected by the concentration of metal ions and sulfide, as well as  $O_2$  exposure during stor-

age as summarized in Table 2. The potential effects can be avoided by appropriate sample treatments as described in the following section.

$O_2$  exposure led to a slight transformation of DOM (AC/M increased by 3%) in two months, for which the effect of  $O_2$  exposure on EEMs of DOM could be negligible. Long-term storage over the years could, however, lead to more bias of spectra, especially for DOM enriched in polyphenols sensitive to  $O_2$ . A consistent way of storage, including duration and headspace, is necessary. Attention is needed on major redox-sensitive ions in natural sed-

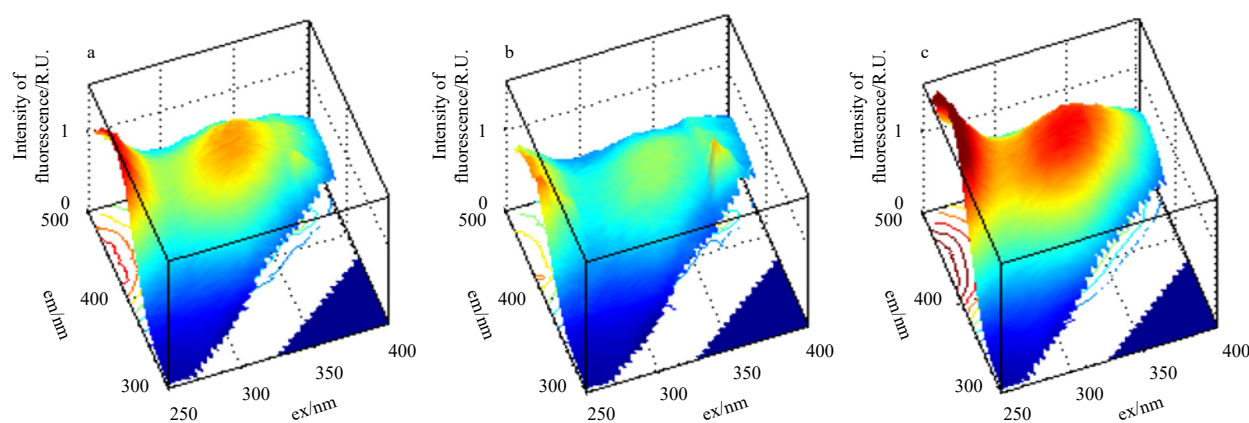


**Fig. 6.** Effect of O<sub>2</sub> exposure on Excitation-Emission Matrix Spectroscopy (EEMs) of pristine sample from Rhône Delta. EEMs of fresh sample without exposure to O<sub>2</sub> (a), exposure to O<sub>2</sub> for 2 h (b) and without precipitation (c). The em and ex represent emission and excitation wavelength, respectively.

**Table 2.** Change of fluorescent signal along with metal ions, sulfide and O<sub>2</sub> exposure. Acceptable ranges of concentrations are listed

Acceptable range	Index	Fe(III) 0–0.007 mmol/L	Fe(II) 0–0.06 mmol/L	Mn(II) 0–0.06 mmol/L	Na <sub>2</sub> S (N <sub>2</sub> -flushed)	Extracted DOM after O <sub>2</sub> exposure 2 months
Bias of 2D index	FI	↑	NS	NS	↑	↓
	HIX	↓	↓	↓	↓	↑
	BIX	↑	NS	NS	↑	NS
Bias of 3D index	protein-like peaks	↓	↓	↓	↑	/
	humic-like peaks	↓	↓	↓	NS	/
	AC/M	↓	↓	↓	↑	NS

Note: The relative changes below 5% were defined as NS, i.e., no significant impact. For 2D index with variation coefficient ranging from 5% to 15%,  $P < 0.05$  in ANOVA were defined as NS. Results of ANOVA are presented in Table S3. ↑ and ↓ represent increase and decrease of the parameters with higher concentrations of added ions or O<sub>2</sub> exposure. FI: fluorescence index; BIX: biological index; HIX: humification index. AC/M: peak height ratio of Peak AC to Peak M.

imentary DOM samples (metal-ion-rich or sulfide-rich). (1) For samples with Fe(II) and Mn(II) concentrations less than 0.7 mmol/L, impacts of both ions are negligible at a dilution factor of 11-fold, final concentration of both ions ( $< 0.06$  mmol/L) are kept; such samples should be stored under N<sub>2</sub> and diluted with O<sub>2</sub>-free water. In the case of inevitable O<sub>2</sub> exposure or storage under air atmosphere, precipitation is likely to occur in the metal-ion-rich pore water samples, and it should be avoided during measurements. Figure 6c showed that after O<sub>2</sub> exposure for 24 h, the EEMs of supernatant of DOM sample emitted more intense fluorescence than that of the original fresh air-free pore water due to exclusion of metal oxide precipitation. (2) Sulfide-rich samples are recommended to be purged with N<sub>2</sub>. Seawater contains ca. 30 mmol/L sulfate. At the oxic and suboxic layer, the sulfide is limited. At the deeper and anoxic layer, the sulfide is usually highly concentrated due to the depletion of oxygen, and sulfate reduction becomes important in the provision of electron acceptors. Therefore, the accumulation of sulfide is very common in the anoxic seafloor. It could reach up to 10 mmol/L in the coastal sediment (Holmer and Kristensen, 1996) and ca. 10–150 μmol/(L·cm<sup>3</sup>) ( $\gg 1$  mmol/L) in the estuarine sediment (Weston et al., 2006). Although the quantitative information of EEMs is similar at 1-mmol/L sulfide without long-term storage, a red shift of the peaks is observable (Fig. 3). Moreover, the sulfide will react with oxygen and after long-term storage sulfur could be formed. The white floccules floating in the sealed vials are not precipitable. They will cause the scattering of signals. Therefore, we recommend either removing the sulfide beforehand or removing the flocculus of sulfur after long-term storage. In the original in-house-prepared North Sea DOM sample, the concentra-

tion of sulfide was 3.95 mmol/L. After purging with N<sub>2</sub> for 2 min, it decreased to 0.01 mmol/L (Table S4). Therefore, removing the sulfide beforehand by purging is an effective way to reduce its impact on fluorescent signals. Alternatively, if the oxidation of sulfide was not avoided, within one week there was 2.06-mmol/L sulfide oxidized to sulfate in the sealed vial and the residual sulfide is only 0.24 mmol/L (Table S4), i.e., theoretically larger than 1-mmol/L sulfide precipitated as elemental sulfur. Unlike the metal oxides, the sulfur precipitates remained in suspension. It is recommended to be excluded via filtration right before the measurement by fluorescence spectroscopy.

It is noteworthy that the signal of protein-like DOM is found to be significantly lost after solid phase extraction. Consequently, the P/H ratio decreased by 60% (Table 3), indicating that the signal of labile DOM might be selectively lost during the extraction

**Table 3.** Comparisons of dissolved organic matter (DOM) fluorescence spectra before and after solid phase extraction (SPE) by pre-cleaned Bond Elut-PPL cartridge

Sample	P/H	AC/M	FI	BIX	HIX
Before SPE-pristine sample	0.5	1.2	1.5	0.9	4.3
After SPE-DOM extract	0.2	1.5	1.6	0.6	8.1
After SPE-residue liquid	1.5	0.6	1.8	1.2	0.5
Standard deviation-pristine sample	0.01	0.01	0.02	0.1	0.2

Note: A 20-mL liquid sample was used for SPE. In-house-prepared samples from the North Sea sediments after incubation were tested since the pristine sample contains both substantial protein-like and humic-like compounds. FI: fluorescence index; BIX: biological index; HIX: humification index. AC/M: peak height ratio of Peaks A and C to Peak M; P/H: peak height ratio of Peak P to Peak H.

process. It suggests caution in comparing EEM and FT-ICR-MS since the pretreatment of the latter includes SPE. If the pore water samples contain a significant fraction of protein-like DOM, the combination of FT-ICR-MS with EEMs is recommended. By the latter technique, information on both protein-like and humic-like DOM is included, and a dataset of hundreds of samples can be easily realized. Based on the overview obtained by EEMs, molecular-level analysis of selected samples by FT-ICR-MS is feasible and provides complementary information.

#### 4 Conclusions

Based on tests of humic-rich SRFA, protein-rich YE and in-house-prepared natural DOM samples, the impacts of various pretreatments of anoxic marine sedimentary pore-water samples were examined: (1) final concentration of Fe(II) and Mn(II) below 0.06 mmol/L is preferred; higher concentrations of Fe(II) and Mn(II) resulted in a noise peak that interfered with PARAFAC analysis and in the substantial loss of fluorescence signal especially for humic-like peaks; DOM samples are most quenched by Fe(III); (2) dissolved sulfide at concentration of 1 mmol/L can cause a slight but observable red-shift of humic-like peaks in SRFA; oxidation of sulfide resulted in sulfur and losses of signals; (3) O<sub>2</sub> exposure slightly changed the EEMs of DOM extracts from in-house-prepared natural samples within two months. Formulae (<1%) located in oxygen-rich polyphenol region in van Krevelen Diagram increased and oxidation of CHOS compounds was observed. Accordingly, the EEMs of extracted DOM was not sensitive to oxygen exposure. For the same pristine water before extraction, however, the EEMs were highly sensitive to oxygen, mainly due to reactions of redox-sensitive ions. More specifically, the metals and sulfides are oxidized and influence their interaction with DOM.

Therefore, we recommend the following measures to reduce the matrix effect on EEMs for the original pore water samples from anoxic marine sediments and SPE is not necessary: (1) storage without headspace of air; sulfide-rich pristine samples should be flushed with N<sub>2</sub> for 2 min to exclude sulfide; (2) dilution with O<sub>2</sub>-free water for pristine marine samples to avoid both the matrix effects and oxidation of metal ions during measurement; (3) measurements of supernatant from pristine samples without precipitation of metal ions or filtrate without floccules if suspended sulfur is formed due to oxidation of sulfide. It should be noted that the oxidation of DOM may be more significant under the long-term storage although the interior change of DOM would not induce bias after two-month exposure of O<sub>2</sub> in this study. For the sedimentary DOM samples examined in this study, microliter volumes (50 μL, ~1 μg C) were sufficient without losses after solid phase extraction, which is a complementary advantage of EEMs combined with FT-ICR-MS analyses. With appropriate pretreatments, EEMs make high-frequency observations possible for anoxic pore water samples from the marine seafloor.

#### Acknowledgements

We thank the captain and crew of R/V *Poseidon* for their excellent support during cruise POS450. Many thanks to the technical assistance of Jenny Wendt and Xavier Prieto Mollar.

#### References

- Albéric P, Sarazin G, Michard G. 1996. Combined amino acid speciation in lake sediment and porewater (Aydat Lake, France). *Aquatic Geochemistry*, 2(1): 29–49, doi: [10.1007/BF00240852](https://doi.org/10.1007/BF00240852)
- Baker A, Bolton L, Newson M, et al. 2008. Spectrophotometric properties of surface water dissolved organic matter in an afforested upland peat catchment. *Hydrological Processes*, 22(13): 2325–2336, doi: [10.1002/hyp.6827](https://doi.org/10.1002/hyp.6827)
- Berner R A. 1982. Burial of organic carbon and pyrite sulfur in the modern ocean: Its geochemical and environmental significance. *American Journal of Science*, 282(4): 451–473, doi: [10.2475/ajs.282.4.451](https://doi.org/10.2475/ajs.282.4.451)
- Berner R A. 1990. Global biogeochemical cycles of carbon and sulfur and atmospheric O<sub>2</sub> over phanerozoic time. *Chemical Geology*, 84(1–4): 159
- Burdige D J. 2001. Dissolved organic matter in Chesapeake Bay sediment pore waters. *Organic Geochemistry*, 32(4): 487–505, doi: [10.1016/S0146-6380\(00\)00191-1](https://doi.org/10.1016/S0146-6380(00)00191-1)
- Burdige D J, Kline S W, Chen Wenhao. 2004. Fluorescent dissolved organic matter in marine sediment pore waters. *Marine Chemistry*, 89(1–4): 289–311, doi: [10.1016/j.marchem.2004.02.015](https://doi.org/10.1016/j.marchem.2004.02.015)
- Canfield D E, Jørgensen B B, Fossing H, et al. 1993. Pathways of organic carbon oxidation in three continental margin sediments. *Marine Geology*, 113(1–2): 27–40, doi: [10.1016/0025-3227\(93\)90147-N](https://doi.org/10.1016/0025-3227(93)90147-N)
- Chen Meilian, Hur J. 2015. Pre-treatments, characteristics, and biogeochemical dynamics of dissolved organic matter in sediments: A review. *Water Research*, 79: 10–25, doi: [10.1016/j.watres.2015.04.018](https://doi.org/10.1016/j.watres.2015.04.018)
- Chin Y P, Traina S J, Swank C R, et al. 1998. Abundance and properties of dissolved organic matter in pore waters of a freshwater wetland. *Limnology and Oceanography*, 43(6): 1287–1296, doi: [10.4319/lo.1998.43.6.1287](https://doi.org/10.4319/lo.1998.43.6.1287)
- Coble P. 2008. Cycling coloured carbon. *Nature Geoscience*, 1(9): 575–576, doi: [10.1038/ngeo294](https://doi.org/10.1038/ngeo294)
- Coble P G. 1996. Characterization of marine and terrestrial DOM in seawater using excitation-emission matrix spectroscopy. *Marine Chemistry*, 51(4): 325–346, doi: [10.1016/0304-4203\(95\)00062-3](https://doi.org/10.1016/0304-4203(95)00062-3)
- Coble P G. 2007. Marine optical biogeochemistry: The chemistry of ocean color. *Chemical Reviews*, 107(2): 402–418, doi: [10.1021/cr050350+](https://doi.org/10.1021/cr050350+)
- Cuss C W, Guéguen C. 2016. Analysis of dissolved organic matter fluorescence using self-organizing maps: mini-review and tutorial. *Analytical Methods*, 8(4): 716–725, doi: [10.1039/C5AY02549D](https://doi.org/10.1039/C5AY02549D)
- De Filippis P, Scarsella M. 2003. Oxidative desulfurization: Oxidation reactivity of sulfur compounds in different organic matrices. *Energy and Fuels*, 17(6): 1452–1455, doi: [10.1021/ef0202539](https://doi.org/10.1021/ef0202539)
- Dittmar T, Koch B, Hertkorn N, et al. 2008. A simple and efficient method for the solid-phase extraction of dissolved organic matter (SPE-DOM) from seawater. *Limnology and Oceanography: Methods*, 6(6): 230–235, doi: [10.4319/lom.2008.6.230](https://doi.org/10.4319/lom.2008.6.230)
- Fellman J B, Hood E, Spencer R G M. 2010. Fluorescence spectroscopy opens new windows into dissolved organic matter dynamics in freshwater ecosystems: A review. *Limnology and Oceanography*, 55(6): 2452–2462, doi: [10.4319/lo.2010.55.6.2452](https://doi.org/10.4319/lo.2010.55.6.2452)
- Gan Shuchai, Schmidt F, Heuer V B, et al. 2020. Impacts of redox conditions on dissolved organic matter (DOM) quality in marine sediments off the River Rhône, Western Mediterranean Sea. *Geochimica et Cosmochimica Acta*, 276: 151–169, doi: [10.1016/j.gca.2020.02.001](https://doi.org/10.1016/j.gca.2020.02.001)
- Gan Shuchai, Wu Ying, Zhang Jing. 2016. Bioavailability of dissolved organic carbon linked with the regional carbon cycle in the East China Sea. *Deep-Sea Research Part II: Topical Studies in Oceanography*, 124: 19–28, doi: [10.1016/j.dsr2.2015.06.024](https://doi.org/10.1016/j.dsr2.2015.06.024)
- Guillemette F, von Wachenfeldt E, Kothawala D N, et al. 2017. Preferential sequestration of terrestrial organic matter in boreal lake sediments. *Journal of Geophysical Research: Biogeosciences*, 122(4): 863–874, doi: [10.1002/2016JG003735](https://doi.org/10.1002/2016JG003735)
- Guo Weidong, Xu Jing, Wang Jiangping, et al. 2010. Characterization of dissolved organic matter in urban sewage using excitation emission matrix fluorescence spectroscopy and parallel factor analysis. *Journal of Environmental Sciences*, 22(11): 1728–1734, doi: [10.1016/S1001-0742\(09\)60312-0](https://doi.org/10.1016/S1001-0742(09)60312-0)
- Hansen A M, Kraus T E C, Pellerin B A, et al. 2016. Optical properties

- of dissolved organic matter (DOM): Effects of biological and photolytic degradation. *Limnology and Oceanography*, 61(3): 1015–1032, doi: [10.1002/lno.10270](https://doi.org/10.1002/lno.10270)
- Hedges J I, Keil R G. 1995. Sedimentary organic matter preservation: an assessment and speculative synthesis. *Marine Chemistry*, 49(2–3): 81–115, doi: [10.1016/0304-4203\(95\)00008-F](https://doi.org/10.1016/0304-4203(95)00008-F)
- Heuer V B, Aiello I W, Elvert M, et al. 2014. Report and preliminary results of R/V *POSEIDON* cruise POS450, DARCSEAS II—Deep subseafloor Archaea in the Western Mediterranean Sea: Carbon Cycle, Life Strategies, and Role in Sedimentary Ecosystems, Barcelona (Spain)—Malaga (Spain), April 2–13, 2013. *Berichte, MARUM—Zentrum für Marine Umweltwissenschaften, Fachbereich Geowissenschaften, Universität Bremen*. 305: 42
- Heuer V B, Pohlman J W, Torres M E, et al. 2009. The stable carbon isotope biogeochemistry of acetate and other dissolved carbon species in deep subseafloor sediments at the northern Cascadia Margin. *Geochimica et Cosmochimica Acta*, 73(11): 3323–3336, doi: [10.1016/j.gca.2009.03.001](https://doi.org/10.1016/j.gca.2009.03.001)
- Holmer M, Kristensen E. 1996. Seasonality of sulfate reduction and pore water solutes in a marine fish farm sediment: the importance of temperature and sedimentary organic matter. *Biogeochemistry*, 32(1): 15–39, doi: [10.1007/BF00001530](https://doi.org/10.1007/BF00001530)
- Huang Shuangbing, Wang Yanxin, Ma Teng, et al. 2015. Linking groundwater dissolved organic matter to sedimentary organic matter from a fluvio-lacustrine aquifer at Jiangnan Plain, China by EEM-PARAFAC and hydrochemical analyses. *Science of the Total Environment*, 529: 131–139, doi: [10.1016/j.scitotenv.2015.05.051](https://doi.org/10.1016/j.scitotenv.2015.05.051)
- Huguet A, Vacher L, Relexans S, et al. 2009. Properties of fluorescent dissolved organic matter in the Gironde Estuary. *Organic Geochemistry*, 40(6): 706–719, doi: [10.1016/j.orggeochem.2009.03.002](https://doi.org/10.1016/j.orggeochem.2009.03.002)
- Ishii S K L, Boyer T H. 2012. Behavior of reoccurring PARAFAC components in fluorescent dissolved organic matter in natural and engineered systems: A critical review. *Environmental Science and Technology*, 46(4): 2006–2017, doi: [10.1021/es2043504](https://doi.org/10.1021/es2043504)
- Jiang Fenghua, Yang Baijuan, Lee Frank Sen-Chun, et al. 2009. Multivariate analysis of fluorescence and source identification of dissolved organic matter in Jiaozhou Bay, China. *Acta Oceanologica Sinica*, 28(2): 60–72
- Koch B P, Dittmar T. 2006. From mass to structure: An aromaticity index for high-resolution mass data of natural organic matter. *Rapid Communications in Mass Spectrometry*, 20(5): 926–932, doi: [10.1002/rcm.2386](https://doi.org/10.1002/rcm.2386)
- Koch B P, Dittmar T. 2016. From mass to structure: An aromaticity index for high-resolution mass data of natural organic matter. *Rapid Communications in Mass Spectrometry*, 30(1): 250, doi: [10.1002/rcm.7433](https://doi.org/10.1002/rcm.7433)
- Komada T, Schofield O M E, Reimers C E. 2002. Fluorescence characteristics of organic matter released from coastal sediments during resuspension. *Marine Chemistry*, 79(2): 81–97, doi: [10.1016/S0304-4203\(02\)00056-7](https://doi.org/10.1016/S0304-4203(02)00056-7)
- Krom M D, Sholkovitz E R. 1977. Nature and reactions of dissolved organic matter in the interstitial waters of marine sediments. *Geochimica et Cosmochimica Acta*, 41(11): 1565–1574, doi: [10.1016/0016-7037\(77\)90168-5](https://doi.org/10.1016/0016-7037(77)90168-5)
- Lin H T, Cowen J P, Olson E J, et al. 2012. Inorganic chemistry, gas compositions and dissolved organic carbon in fluids from sedimented young basaltic crust on the Juan de Fuca Ridge flanks. *Geochimica et Cosmochimica Acta*, 85: 213–227, doi: [10.1016/j.gca.2012.02.017](https://doi.org/10.1016/j.gca.2012.02.017)
- Lin H T, Hsieh C C, Cowen J P, et al. 2015. Data report: dissolved and particulate organic carbon in the deep sediments of IODP Site U1363 near Grizzly Bare seamount. In: *Proceedings of the Integrated Ocean Drilling Program, Volume 327*. Tokyo: Integrated Ocean Drilling Program Management International, Inc., doi: [10.2204/iodp.proc.327.202.2015](https://doi.org/10.2204/iodp.proc.327.202.2015)
- Lin Y S, Koch B P, Feseker T, et al. 2017. Near-surface heating of young rift sediment causes mass production and discharge of reactive dissolved organic matter. *Scientific Reports*, 7(1): 44864, doi: [10.1038/srep44864](https://doi.org/10.1038/srep44864)
- Lomstein B A, Jensen A G U, Hansen J W, et al. 1998. Budgets of sediment nitrogen and carbon cycling in the shallow water of Knebel Vig, Denmark. *Aquatic Microbial Ecology*, 14(1): 69–80, doi: [10.3354/ame014069](https://doi.org/10.3354/ame014069)
- Lønborg C, Álvarez-Salgado X A, Davidson K, et al. 2010. Assessing the microbial bioavailability and degradation rate constants of dissolved organic matter by fluorescence spectroscopy in the coastal upwelling system of the Ría de Vigo. *Marine Chemistry*, 119(1–4): 121–129, doi: [10.1016/j.marchem.2010.02.001](https://doi.org/10.1016/j.marchem.2010.02.001)
- Manciulea A, Baker A, Lead J R. 2009. A fluorescence quenching study of the interaction of Suwannee River fulvic acid with iron oxide nanoparticles. *Chemosphere*, 76(8): 1023–1027, doi: [10.1016/j.chemosphere.2009.04.067](https://doi.org/10.1016/j.chemosphere.2009.04.067)
- McKnight D M, Boyer E W, Westerhoff P K, et al. 2001. Spectrofluorometric characterization of dissolved organic matter for indication of precursor organic material and aromaticity. *Limnology and Oceanography*, 46(1): 38–48, doi: [10.4319/lo.2001.46.1.0038](https://doi.org/10.4319/lo.2001.46.1.0038)
- Middelburg J J, Vlug T, Jaco F, et al. 1993. Organic matter mineralization in marine systems. *Global and Planetary Change*, 8(1–2): 47–58, doi: [10.1016/0921-8181\(93\)90062-S](https://doi.org/10.1016/0921-8181(93)90062-S)
- Moini M, Jones B L, Rogers R M, et al. 1998. Sodium trifluoroacetate as a tune/calibration compound for positive- and negative-ion electrospray ionization mass spectrometry in the mass range of 100–4000 Da. *Journal of the American Society for Mass Spectrometry*, 9(9): 977–980, doi: [10.1016/S1044-0305\(98\)00079-8](https://doi.org/10.1016/S1044-0305(98)00079-8)
- Murphy K R, Butler K D, Spencer R G M, et al. 2010. Measurement of dissolved organic matter fluorescence in aquatic environments: An interlaboratory comparison. *Environmental Science & Technology*, 44(24): 9405–9412, doi: [10.1021/es102362t](https://doi.org/10.1021/es102362t)
- Murphy K R, Stedmon C A, Wenig P, et al. 2014. OpenFluor—an online spectral library of auto-fluorescence by organic compounds in the environment. *Analytical Methods*, 6(3): 658–661, doi: [10.1039/C3AY41935E](https://doi.org/10.1039/C3AY41935E)
- Murphy K R, Stedmon C A, Graeber D, et al. 2013. Fluorescence spectroscopy and multi-way techniques. PARAFAC. *Analytical Methods*, 5(23): 6557–6566, doi: [10.1039/c3ay41160e](https://doi.org/10.1039/c3ay41160e)
- Ohno T. 2002. Fluorescence inner-filtering correction for determining the humification index of dissolved organic matter. *Environmental Science and Technology*, 36(4): 742–746, doi: [10.1021/es0155276](https://doi.org/10.1021/es0155276)
- Poncet-Legrand C, Cabane B, Bautista-Ortín A B, et al. 2010. Tannin oxidation: Intra-versus intermolecular reactions. *Biomacromolecules*, 11(9): 2376–2386, doi: [10.1021/bm100515e](https://doi.org/10.1021/bm100515e)
- Poulin B A, Ryan J N, Aiken G R. 2014. Effects of iron on optical properties of dissolved organic matter. *Environmental Science and Technology*, 48(17): 10098–10106, doi: [10.1021/es502670r](https://doi.org/10.1021/es502670r)
- Rennert T, Gockel K F, Mansfeldt T. 2007. Extraction of water-soluble organic matter from mineral horizons of forest soils. *Journal of Plant Nutrition and Soil Science*, 170(4): 514–521, doi: [10.1002/jpln.200625099](https://doi.org/10.1002/jpln.200625099)
- Schmidt F, Elvert M, Koch B P, et al. 2009. Molecular characterization of dissolved organic matter in pore water of continental shelf sediments. *Geochimica et Cosmochimica Acta*, 73(11): 3337–3358, doi: [10.1016/j.gca.2009.03.008](https://doi.org/10.1016/j.gca.2009.03.008)
- Schmidt F, Koch B P, Elvert M, et al. 2011. Diagenetic transformation of dissolved organic nitrogen compounds under contrasting sedimentary redox conditions in the black sea. *Environmental Science and Technology*, 45(12): 5223–5229, doi: [10.1021/es2003414](https://doi.org/10.1021/es2003414)
- Schmidt F, Koch B P, Goldhammer T, et al. 2017. Unraveling signatures of biogeochemical processes and the depositional setting in the molecular composition of pore water DOM across different marine environments. *Geochimica et Cosmochimica Acta*, 207: 57–80, doi: [10.1016/j.gca.2017.03.005](https://doi.org/10.1016/j.gca.2017.03.005)
- Schmidt F, Koch B P, Witt M, et al. 2014. Extending the analytical window for water-soluble organic matter in sediments by aqueous Soxhlet extraction. *Geochimica et Cosmochimica Acta*, 141: 83–96, doi: [10.1016/j.gca.2014.06.009](https://doi.org/10.1016/j.gca.2014.06.009)
- Schulz H D, Dahmke A, Schinzel U, et al. 1994. Early diagenetic processes, fluxes, and reaction rates in sediments of the South Atlantic. *Geochimica et Cosmochimica Acta*, 58(9): 2041–2060,

- doi: [10.1016/0016-7037\(94\)90284-4](https://doi.org/10.1016/0016-7037(94)90284-4)
- Senesi N, Miano T M, Provenzano M R, et al. 1991. Characterization, differentiation, and classification of humic substances by fluorescence spectroscopy. *Soil Science*, 152(4): 259–271, doi: [10.1097/00010694-199110000-00004](https://doi.org/10.1097/00010694-199110000-00004)
- Simoneit B R T, Sparrow M A. 2002. Dissolved organic carbon in interstitial waters from sediments of Middle Valley and Escanaba Trough, Northeast Pacific, ODP Legs 139 and 169. *Applied Geochemistry*, 17(11): 1495–1502, doi: [10.1016/S0883-2927\(02\)00114-2](https://doi.org/10.1016/S0883-2927(02)00114-2)
- Stedmon C A, Bro R. 2008. Characterizing dissolved organic matter fluorescence with parallel factor analysis: A tutorial. *Limnology and Oceanography: Methods*, 6(11): 572–579, doi: [10.4319/lom.2008.6.572](https://doi.org/10.4319/lom.2008.6.572)
- Stedmon C A, Markager S. 2005. Resolving the variability in dissolved organic matter fluorescence in a temperate estuary and its catchment using PARAFAC analysis. *Limnology and Oceanography*, 50(2): 686–697, doi: [10.4319/lo.2005.50.2.0686](https://doi.org/10.4319/lo.2005.50.2.0686)
- Tfaily M M, Hamdan R, Corbett J E, et al. 2013. Investigating dissolved organic matter decomposition in northern peatlands using complimentary analytical techniques. *Geochimica et Cosmochimica Acta*, 112: 116–129, doi: [10.1016/j.gca.2013.03.002](https://doi.org/10.1016/j.gca.2013.03.002)
- Valle J, Gonsior M, Harir M, et al. 2018. Extensive processing of sediment pore water dissolved organic matter during anoxic incubation as observed by high-field mass spectrometry (FTICR-MS). *Water Research*, 129: 252–263, doi: [10.1016/j.watres.2017.11.015](https://doi.org/10.1016/j.watres.2017.11.015)
- Wang Xiaona, Wu Ying, Bao Hongyan, et al. 2019. Sources, transport, and transformation of dissolved organic matter in a large river system: Illustrated by the Changjiang River, China. *Journal of Geophysical Research: Biogeosciences*, 124(12): 3881–3901, doi: [10.1029/2018JG004986](https://doi.org/10.1029/2018JG004986)
- Weston N B, Porubsky W P, Samarkin V A, et al. 2006. Porewater stoichiometry of terminal metabolic products, sulfate, and dissolved organic carbon and nitrogen in estuarine intertidal creek-bank sediments. *Biogeochemistry*, 77(3): 375–408, doi: [10.1007/s10533-005-1640-1](https://doi.org/10.1007/s10533-005-1640-1)
- Wolfe A P, Kaushal S S, Fulton J R, et al. 2002. Spectrofluorescence of sediment humic substances and historical changes of lacustrine organic matter provenance in response to atmospheric nutrient enrichment. *Environmental Science and Technology*, 36(15): 3217–3223, doi: [10.1021/es011215r](https://doi.org/10.1021/es011215r)
- Wu Weichao, Meador T, Hinrichs K U. 2018. Production and turnover of microbial organic matter in surface intertidal sediments. *Organic Geochemistry*, 121: 104–113, doi: [10.1016/J.ORGGEOCHEM.2018.04.006](https://doi.org/10.1016/J.ORGGEOCHEM.2018.04.006)
- Yamashita Y, Jaffé R, Maie N, et al. 2008. Assessing the dynamics of dissolved organic matter (DOM) in coastal environments by excitation emission matrix fluorescence and parallel factor analysis (EEM-PARAFAC). *Limnology and Oceanography*, 53(5): 1900–1908, doi: [10.4319/lo.2008.53.5.1900](https://doi.org/10.4319/lo.2008.53.5.1900)
- Yamashita Y, Tanoue E. 2003. Chemical characterization of protein-like fluorophores in DOM in relation to aromatic amino acids. *Marine Chemistry*, 82(3–4): 255–271, doi: [10.1016/S0304-4203\(03\)00073-2](https://doi.org/10.1016/S0304-4203(03)00073-2) doi: [10.1016/S0304-4203\(03\)00073-2](https://doi.org/10.1016/S0304-4203(03)00073-2)
- Yi Yueyuan, Zheng Airong, Guo Weidong, et al. 2014. Optical properties of estuarine dissolved organic matter isolated using cross-flow ultrafiltration. *Acta Oceanologica Sinica*, 33(4): 22–29, doi: [10.1007/s13131-014-0451-4](https://doi.org/10.1007/s13131-014-0451-4)
- Zhuang Guang-Chao, Lin Yu-Shih, Elvert M, et al. 2014. Gas chromatographic analysis of methanol and ethanol in marine sediment pore waters: Validation and implementation of three pretreatment techniques. *Marine Chemistry*, 160: 82–90, doi: [10.1016/j.marchem.2014.01.011](https://doi.org/10.1016/j.marchem.2014.01.011)
- Zsolnay A, Baigar E, Jimenez M, et al. 1999. Differentiating with fluorescence spectroscopy the sources of dissolved organic matter in soils subjected to drying. *Chemosphere*, 38(1): 45–50, doi: [10.1016/S0045-6535\(98\)00166-0](https://doi.org/10.1016/S0045-6535(98)00166-0)

## Supplementary information:

**Fig. S1.** Frame diagram of all the subseries experiments.

**Fig. S2.** Validation of PARAFAC analysis by split-half analysis.

**Fig. S3.** Match of emission spectra in the PARAFAC model against the online library ([www.OpenFluor.com](http://www.OpenFluor.com)).

**Fig. S4.** Impact of concentration of SRFA on index derived from humic-like peaks: peaks intensity (a), 3D and 2D index (b).

**Fig. S5.** Impact of 11-times dilution on index derived from humic-like peaks. Black column: Rhône Delta; red column: North Sea.

**Table S1.** Peaks identified in this study.

**Table S2.** Original dataset and derived parameters after PARAFAC analysis.

**Table S3.** Significance analysis by ANOVA (significance level=0.05). Change of fluorescent signal along with NaCl concentration, metal ions and sulfide exposure.

**Table S4.** Variation of sulfide and sulfate after treatments of N<sub>2</sub>-flushing and O<sub>2</sub> exposure. In-house-prepared samples from North Sea sediments were tested.

The supplementary information is available online at <https://doi.org/10.1007/s13131-022-2050-0> and <http://www.aosocean.com/>. The supplementary information is published as submitted, without typesetting or editing. The responsibility for scientific accuracy and content remains entirely with the authors.